Bioresource Technology 380 (2023) 129086

Contents lists available at ScienceDirect

Bioresource Technology

journal homepage: www.elsevier.com/locate/biortech

Simulation of anaerobic co-digestion of steam explosion pulping wastewater with cattle manure: Focusing on degradation and inhibition of furfural

Pengfei Li [a,b,1], Xinyu Wei [c,1], Ming Wang [d,1], Di Liu [a], Jie Liu [a,b,*], Zhanjiang Pei [b], Fengmei Shi [b], Su Wang [b], Xin Zuo [b], Dan Li [b], Hongjiu Yu [b], Nan Zhang [b], Qiuyue Yu [b], Yifei Luo [b]

[a] Heilongjiang Academy of Agricultural Sciences Postdoctoral Workstation, Harbin 150086, PR China
[b] Heilongjiang Academy of Black Soil Conservation and Utilization, Key Laboratory Combining Farming & Animal Husbandry, Key Laboratory of Straw Energy Utilization, Harbin 150086, PR China
[c] Rural Energy and Environment Agency, Ministry of Agriculture and Rural Affairs, Beijing 100125, PR China
[d] Department of Agriculture Biological Environment and Energy Engineering, School of Engineering, Northeast Agriculture University, Harbin 150030, PR China

HIGHLIGHTS

- Batch and semi-continuous co-digestion of CM and SEPW were implemented.
- A modified ADM1 containing furfural degradation process was established.
- Furoic acid was introduced as an intermediate in furfural degradation.
- Modified ADM1 was used to simulate batch and semi-continuous AD.
- Furfural tolerance of batch and semi-continuous systems were evaluated.

GRAPHICAL ABSTRACT

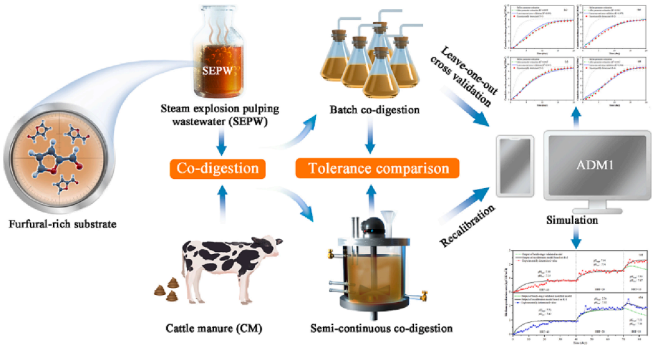

ARTICLE INFO

Keywords:
Anaerobic digestion
Furfural inhibition
Cross-validation
Model recalibration

ABSTRACT

In this study, an extended Anaerobic Digestion Model No.1, which considered the degradation and inhibition properties of furfural, was established and implemented to simulate the anaerobic co-digestion of steam explosion pulping wastewater and cattle manure in batch and semi-continuous modes. Batch and semi-continuous experimental data helped calibrate the new model and recalibrate the parameters related to furfural degradation, respectively. The cross-validation results showed the batch-stage calibration model accurately predicted the methanogenic behavior of all experimental treatments ($R^2 \geq 0.959$). Meanwhile, the recalibrated model satisfactorily matched the methane production results in the stable and high furfural loading stages in the semi-continuous experiment. In addition, recalibration results revealed the semi-continuous system tolerated furfural better than the batch system. These results provide insights into the anaerobic treatments and mathematical simulations of furfural-rich substrates.

* Corresponding author at: Heilongjiang Academy of Agricultural Sciences Postdoctoral workstation, Harbin 150086, PR China.
E-mail address: bsculiujie@163.com (J. Liu).
[1] These authors have contributed equally to this work.

https://doi.org/10.1016/j.biortech.2023.129086
Received 10 July 2022; Received in revised form 8 April 2023; Accepted 20 April 2023
Available online 24 April 2023

1. Introduction

Steam explosion pulping (SEP) has been widely utilized in the papermaking industry due to its low energy consumption and chemical usage (Sarker et al., 2021; Yu et al., 2022). Since crop straw is less expensive and more accessible than wood, it is attracting more attention as a potential SEP raw material (Montane et al., 1998; Wang and Chen, 2013). Straw undergoes shear tearing and some autocatalytic degradation due to the flash distillation and explosion of steam in SEP, yielding oligomers and monomer sugars, organic acids, and small molecular products like furfural (Sarker et al., 2021; Boopathy et al., 1993). These products, which are ineffective for papermaking, are extracted during subsequent water extraction and leaching stages and discharged as steam explosion pulping wastewater (SEPW) (Ruiz et al., 2021). The harmless treatment and resource utilization of SEPW are considered core elements for the sustainable development of the SEP industry.

The process of anaerobic digestion (AD) has been widely recognized as a potential method of recycling organic waste. SEPW contains high concentrations of soluble sugars, acetic acid, and a significant quantity of furfural (approximately 2.88 g/L) (Boopathy et al., 1993). Methanogenic microorganisms readily digest soluble sugars and acetic acid via AD, while furfural inhibits methanogen activity that reduces performance at high levels (Ketsub et al., 2022; Li et al., 2022). Previous studies concluded that furfural completely inhibited methanogenic activity at 2.0 g/L under both thermophilic and mesophilic conditions (Ghasimi et al., 2016). High levels of furfural preclude utilizing SEPW as the sole substrate for AD, whereas anaerobic co-digestion with the potential of dilution inhibitor/toxicity may viably address this issue (Karki et al., 2021). Cattle manure (CM) is regarded as an excellent co-substrate and has frequently appeared in co-digestion studies with various wastewater types, including olive mill (Dareioti et al., 2010), wine distillery (Akassou et al., 2010), and petrochemical wastewater (Siddique et al., 2014). However, few studies have examined the feasibility and process characteristics of anaerobic co-digestion of SEPW and CM.

Anaerobic Digestion Model No. 1 (ADM1) is a simulation and modeling tool for the dynamic AD process that can be used to direct the operation and optimization of anaerobic reactors and facilitate understanding of particular phenomena observed (Emebu et al., 2022). Due to the non-negligible furfural levels in SEPW, it is predictable that extending ADM1 to encompass the degradation and inhibition of furfural is fundamental to accurately simulating the anaerobic co-digestion of SEPW and CM. In a kinetic study on the anaerobic treatment of hydrothermally solubilized sugarcane bagasse, Liu et al. (2017) first proposed the uptake of 14 kinds of COD substances, including furfural and hydroxyl-methyl-furfural, into modified ADM1. After that, Raya and Ghimire (2022) expanded ADM1 to include the degradation and inhibition of phenol, furfural, and 5-hydroxymethylfurfural in the AD of aqueous pyrolysis liquids. However, they assumed that furfural degrades directly to acetic acid and hydrogen in both of their modified ADM1 simulations and did not take intermediate processes into account. According to research conducted by Rivard and Grohmann (1991), furfuryl alcohol and furoic acid were found to be critical intermediates in the anaerobic breakdown of furfural to acetic acid. Furfuryl alcohol and furoic acid are much less toxic to methanogenic microorganisms than furfural. Furthermore, the rate of furfural conversion to any intermediate is significantly higher than its conversion to acetic acid (Ghasimi et al., 2016; Sun et al., 2020). Therefore, the introduction of furfuryl alcohol and/or furoic acid into the ADM1 simulation of anaerobic co-digestion of SEPW and CM was necessary to accurately characterize the degradation and inhibitory behavior of furfural and its derivatives to improve confidence in the simulation. However, to the best of our knowledge, a modified ADM1 that accounts for furfuryl alcohol and/or furoic acid as intermediates during the anaerobic conversion of furfural has not been established, with limited information on the relevant kinetic parameters.

This study establishes and implements a modified ADM1 that emphasizes the inhibitory properties and degradation pathways of furfural to simulate batch and semi-continuous anaerobic co-digestion of SEPW and CM. The objectives of this work were: (i) to explore the feasibility of co-digestion of SEWP and CM, (ii) to establish a modified ADM1 capable of accurately modelling the co-digestion of SEPW and CM, (iii) to investigate and clarify the ADM1 degradation kinetic parameters of furfural and its derivatives and (iv) to compare and reveal differences in tolerance to furfural toxicity between batch and semi-continuous AD systems. This research should provide insights into the anaerobic treatments of furfural-rich substrates.

2. Materials and methods

2.1. Substrate and inoculum

Fresh CM was collected from farms in the vicinity of the laboratory (Songbei District, Harbin City, Heilongjiang Province, China). After sieving out debris and larger fibers, CM was placed in the fresh-keeping layer of the refrigerator and stored at 4 °C until use. SEPW was obtained from Heilongjiang Longteng Paper Co., Ltd., which was produced from corn stover under steam explosion conditions of 2.0 MPa and 218–220 °C. SEPW was stored in a sealed flask at 4 °C until use. The inoculum was anaerobic sludge from the biogas project of the Harbin Yunyan Animal Husbandry Science and Technology Park, which has been treating pig manure (organic load rate (OLR) approximately 2.0 kg COD/m^3·d) in mesophilic (36 °C) semi-continuous mode for a long time. The inoculum was degassed for 14 days at 36 °C before AD to allow any residual organics in the inoculum to be digested. Table 1 lists the compositional characteristics of the substrates and inoculum.

2.2. Analytical methods

Total solids (TS), volatile solids (VS), pH (Sartorius basic pH meter PB-10, Germany), volatile suspended solids (VSS), COD and total Kjeldahl nitrogen (TKN) were determined according to standard methods (APHA, 2005). Kjeldahl nitrogen ×6.25 was used as the crude protein content (Girolamo et al., 2013). Soluble sugars in SEPW were

Table 1
Composition characteristics of the substrates and inoculum.

Item	Unit	Types of substrates		
		SEPW	CM	Inoculum
TS	%	1.95(0.02)	18.11(0.10)	2.10(0.05)
VS	%TS	90.29(1.05)	81.72(0.99)	52.65(0.64)
pH	–	4.24(0.01)	7.85(0.02)	7.26(0.01)
VSS	g/L	–	–	3.93(0.04)
TCOD	g/L	25.39(1.20)	–	–
Soluble sugars	g/L	13.64(0.53)	–	–
Furfural	g/L	4.61(0.13)	–	–
5-Hydroxymethylfurfural	mg/L	6.32(0.12)	–	–
Acetic acid	g/L	2.05(0.04)	–	–
Propionic acid	g/L	0.09(0.02)	–	–
Butyric acid	g/L	0.13(0.01)	–	–
Ash	%TS	9.61(0.23)	18.28(0.42)	–
Crude protein	%TS	–	8.63(0.30)	–
Crude fat	%TS	–	3.66(0.28)	–
Starch[a]	%TS	–	12.57(1.05)	–
Hemicellulose	%TS	–	24.43(1.22)	–
Cellulose	%TS	–	20.91(0.69)	–
Lignin	%TS	–	11.52(0.38)	–
NDF removal[b]	%	–	42.36(2.19)	–

Note: TS (total solids), TS (volatile solids), VSS (volatile suspended solids), TCOD (total chemical oxygen demand), and NDF (neutral detergent fiber); each of the indicators was measured three times, and the average value was taken.

[a] Calculated by subtracting the sum of the hemicellulose, cellulose, lignin, crude protein, and crude fat contents from the VS content, which mainly consisted of starch or easily degradable sugars.

[b] Average neutral detergent fiber removal for T-1, −2, −3, and −4.

determined using the Fehling reagent method (Lane and Eynon, 1924). UV absorbance values (Shimadzu UV3600, Japan) at 277 and 285 nm determined the furfural and 5-hydroxymethylfurfural levels in SEPW as described by Chi et al. (2009). An Agilent GC-6800 N chromatograph (Agilent Inc., Santa Clara, CA, USA) determined biogas composition and volatile organic acids (VFAs). Crude fat contents were determined using Soxhlet extraction. Hemicellulose, cellulose, and lignin contents were determined using an ANKOM A200i fiber analyzer (ANKOM Technology, Macedon, NY, USA) according to Koch et al. (2010). Each indicator was measured three times and averaged.

2.3. Design of batch and semi-continuous experiments

2.3.1. Batch experiments

The four mixing ratios based on wet weight (dry weight) of SEPW and CM for co-digestion were 1:4 (1:37), 2:4 (2:37), 3:4 (3:37), and 4:4 (4:37), respectively numbered as MR-1, −2, −3, and −4. Distilled water was added to make up the SEPW difference to ensure equal mass in each co-substrate ratio. The pH of the SEPW was adjusted to 7.0±0.1 using 0.2 M NaOH before mixing. Four treatments using MR-1 (T-1), MR-2 (T-2), MR-3 (T-3), and MR-4 (T-4) as substrates, and a control treatment ($T_{control}$) were set up in the batch-stage. Each treatment was performed in triplicate. 635 g of inoculum, 160 g of mixed co-substrate (in $T_{control}$, replace with 160 g distilled water) and 5 mL of elemental supplement solution (prepared in advance according to Monlau et al. (2012)) were added to a 1.0 L flask to obtain a working volume of 0.8 L. The VS-based substrate to inoculum ratios of T-1, T-2, T-3, and T-4 were 1.74, 1.79, 1.84, and 1.89 g VS/g VS, respectively. After purging the headspace with N_2 for 3 min, all flasks were sealed and connected to aluminum gas collection bags using rubber tubing. The flasks were put in a constant temperature incubator at 36±1 °C. Flasks were shaken manually for 1 min after measuring the biogas volume and composition daily. The biogas volume measured using the water displacement method (see supplementary material) was converted to the volume under standard conditions (273 K, 1.00 atm) by Kafle and Kim (2012).

2.3.2. Semi-continuous experiments

Mesophilic semi-continuous experiments (36±1 °C) were carried out in self-designed plexiglass AD reactors with automatic temperature control and stirring. MR-2, with a medium furfural concentration, and MR-4, with the maximum furfural concentration, were selected as substrates in this stage to explore the tolerance limit of the semi-continuous system to the toxicity of furfural and ensure the experimental data sources used for model calibration and validation differed sufficiently. Two identical reactors, R-1 (with MR-2 as the substrate) and R-2 (with MR-4 as the substrate) were simultaneously set up and operated. Both reactors had a total volume of 10 L and a working volume of 8 L. The semi-continuous mode was achieved by the daily removal of digestate from a discharge port located in the lower part of the reactor, followed by the addition of the substrate from a feed port located at the top of the reactor. Both reactors were stirred for 5 min at 60 rpm once every 24 h to enhance mass transfer and promote contact between the microorganisms and nutrients. The semi-continuous experiment was divided into three phases according changes in hydraulic retention time (HRT); R-1 and R-2 were run at the same HRT throughout. In the first phase, an initial HRT of 40 days (OLR 2.65 g COD/(L·d) for R-1 and 2.81 g COD/(L·d) for R-2) carried out for 40 days to enable initiation of experiments and microorganism acclimation. After 40 days, the HRT was adjusted to 20 days (OLR 5.30 g COD/(L·d) for R-1 and 5.62 g COD/(L·d) for R-2) for 30 days in the second phase. The HRT was again reduced to 10 days (OLR 10.60 g COD/(L·d) for R-1 and 11.23 g COD/(L·d) for R-2) and continued until the end of the experiment. Ensure that both reactors reach steady state at each phase (methane production fluctuated no more than 10% in one week) (Zhao et al., 2019). The biogas volume from the gas flowmeter and the pH of the digestate was recorded daily during the semi-continuous experiments.

2.4. Model modification and model implementation

2.4.1. Model modifications

According to Shi et al. (2014), CM fractionates into four parts after disintegration—the inert fraction (contains lignin), the protein fraction, the readily hydrolyzable fraction (RHF, contains starch), and the slowly hydrolyzable fraction (SHF, contains cellulose and hemicellulose). Sugar-degrading bacteria hydrolyze RHF and SHF at different rates, producing soluble sugar (Li et al., 2021). The crude fat content in CM was low (3.66% of TS), and therefore, this fraction was ignored for simplification. Regarding the modification of the SEPW section, bacteria can absorb soluble sugars and VFAs without hydrolysis, whereas furfural was degraded into acetic acid and hydrogen via a stepwise alcohol-aldehyde-acid sequence. In particular, research by Rivard and Grohmann (1991) indicated that, despite being a genuine intermediate in furfural degradation, the concentration of furfuryl alcohol in furfural anaerobic degradation systems remained low because of rapid conversion into furoic acid. Therefore, only furoic acid was included as an intermediate for furfural degradation in the modified version of ADM1 established in this study. In contrast, the concentrations of 5-hydroxymethylfurfural, propionic acid, and butyric acid in SEPW were relatively low and were omitted to simplify the model. The above modifications have been added to the new ADM1 metabolic pathway (see supplementary material).

The uptake rates of furfural and acetic acid were adapted to account for the toxicity of high furfural concentrations to microorganisms. Furfural uptake was described using the Haldane growth kinetic equation, which illustrates the growth inhibition of substrates on microorganisms (Chai et al., 2021). A non-competitive form of inhibition control was added to acetate uptake to characterize repression of the acetate-methanogenic metabolic pathway by high furfural levels (Fezzani and Cheikh, 2009; Raya and Ghimire, 2022). The process matrix corresponding to the modified conversion pathway is shown in Table 2.

Table 2
Process matrix for COD conservation in modified models.

Process	X_C	X_{pr}	X_{RHF}	X_{SHF}	X_I	S_{su}	S_{fu}	S_{fua}	S_{ac}	S_{h2}	S_{ch4}	X_{ac}	X_{fu}	Rate (kgCOD/m^{3}d)
1. Disintegration of CM	−1	$f_{pr,C}$	$f_{RHF,C}$	$f_{SHF,C}$	$f_{i,C}$									$k_{dis}X_C$
2. Hydrolysis of RHF			−1		$f_{i,RHF}$	$f_{su,RHF}$								$k_{hyd,RHF}\frac{X_{RHF}}{K_{hyd,RHF}X_{su}+X_{RHF}}X_{su}$
3. Hydrolysis of SHF				−1	$f_{i,SHF}$	$f_{su,SHF}$								$k_{hyd,SHF}\frac{X_{SHF}}{K_{hyd,SHF}X_{su}+X_{SHF}}X_{su}$
4. Uptake of furfural							−1	$f_{fua,fu}$					Y_{fu}	$k_{m,fu}\frac{S_{fu}}{K_{s,fu}+(S_{fu})^2/K_{I,fu}}X_{fu}$
5. Uptake of furoic acid								−1	$f_{ac,fua}$	$f_{h2,fua}$			Y_{fu}	$k_{m,fua}\frac{S_{fua}}{K_{s,fua}+S_{fua}}X_{fu}$
6. Uptake of acetic acid									−1		(1-Y_{ac})	Y_{ac}		$k_{m,ac}\frac{S_{ac}}{K_{s,ac}+S_{ac}}X_{ac}\frac{1}{1+S_{fu}/K_{I,fu}}$
7. Decay of furfural biomass	1												−1	$k_{dec,fu}X_{fu}$

Note: Only the modified process matrix sections are listed.

2.4.2. Initial state variables for model input

According to Koch et al. (2010), the theoretical COD (thCOD) of CM and organic matter in SEPW were calculated using Eqs. (1) and (2):

$$\mathrm{thCOD_{CM}} = \left(\frac{(\mathrm{st}+\mathrm{hem}+\mathrm{cel})\times 1.19+\mathrm{pr}\times 1.42+\mathrm{lig}\times 1.56}{100}\right)\mathrm{kgO_2/kgTS} \quad (1)$$

$$\mathrm{thCOD\ of\ C_aH_bO_c} = \left(\frac{(\mathrm{a}\times 2+\mathrm{b}\times 0.5-\mathrm{c})\times 16}{12\mathrm{a}+\mathrm{b}+16\mathrm{c}}\right)\mathrm{kgO_2/kg_{organic}} \quad (2)$$

where st, hem, cel, pr, and lig represent the contents of starch, hemicellulose, cellulose, crude protein, and lignin in CM (% TS). Based on the thCOD of CM (calculated as 1.10 kg O_2/kg TS) and total COD of SEPW (Table 1), the initial substrate concentrations (X_C) in T-1, −2, −3, and −4 reactors were calculated as 20.51, 21.15, 21.78, and 22.42 kg COD/m^3, respectively. The stoichiometric parameters of CM into RHF ($f_{\mathrm{RHF,C}}$), SHF ($f_{\mathrm{SHF,C}}$), protein fraction ($f_{\mathrm{pr,C}}$), and inert fractions ($f_{\mathrm{i,C}}$) were 0.20, 0.55, 0.11, and 0.14, according to Li et al. (2021). The yield of soluble sugars to SHF ($f_{\mathrm{su,SHF}}$) was calculated based on experimentally determined NDF removal degree in the batch-stage, as shown in Eq. (3):

$$f_{\mathrm{su,SHF}} = \frac{(\mathrm{NDF}\times \mathrm{R_{NDF}})}{(\mathrm{hem}+\mathrm{cel})}\left[\frac{\%}{\%}\right] \quad (3)$$

where R_{NDF} is the NDF removal degree (Table 1). Next, the yield of inert components to SHF ($f_{\mathrm{i,SHF}}$) was calculated as "1 – $f_{\mathrm{su,SHF}}$". Microorganisms release two units of acetic acid and one unit of hydrogen for each unit of furoic acid uptake; thus, the yield of acetic acid ($f_{\mathrm{ac,fua}}$) and H_2 ($f_{\mathrm{h2,fua}}$) to furoic acid was calculated using Eqs. (4) and (5):

$$f_{\mathrm{ac,fua}} = (1-Y_{\mathrm{fu}})\left(\frac{\mathrm{thCOD_{ac}}\times 2}{\mathrm{thCOD_{ac}}\times 2+\mathrm{thCOD_{h2}}}\right) \quad (4)$$

$$f_{\mathrm{h2,fua}} = (1-Y_{\mathrm{fu}})\left(\frac{\mathrm{thCOD_{h2}}}{\mathrm{thCOD_{ac}}\times 2+\mathrm{thCOD_{h2}}}\right) \quad (5)$$

where Y_{fu} represents the yield of furfural degrading bacteria to furoic acid. Calculations yielded $f_{\mathrm{su,SHF}}$, $f_{\mathrm{i,SHF}}$, $f_{\mathrm{ac,fua}}$, and $f_{\mathrm{h2,fua}}$ values of 0.53, 0.47, 0.82, and 0.10, respectively. According to Zhao et al. (2009), the fractions of sugar ($f_{\mathrm{su,RHF}}$) and inert ($f_{\mathrm{i,RHF}}$) from RHF were assigned 0.95 and 0.05, respectively. The fraction of furoic acid ($f_{\mathrm{fua,fu}}$), inert ($f_{\mathrm{i,fu}}$), and furfural degraders (Y_{fu}) from furfural uptake are 0.74, 0.18, and 0.08, respectively, as Rivard and Grohmann (1991) and Raya and Ghimire (2022) reported.

The initial value of disintegration rate coefficient of CM (k_{dis}, 0.50 d^{-1}), hydrolysis rate constants of RHF ($k_{\mathrm{hyd,RHF}}$, 9.68 d^{-1}) and SHF ($k_{\mathrm{hyd,SHF}}$, 2.41 d^{-1}), hydrolysis saturation constants of RHF ($K_{\mathrm{hyd,RHF}}$, 0.05 kg COD/m^3) and SHF ($K_{\mathrm{hyd,SHF}}$, 0.05 kg COD/m^3) were obtained from Shi et al. (2014) and Zhao et al. (2009). For the kinetic parameters related to the degradation of furfural and furoic acid, except that the initial values of maximum specific uptake rate of furoic acid ($k_{\mathrm{m,fua}}$) and half-saturation coefficient of furoic acid ($K_{\mathrm{s,fua}}$) cannot be found in the literature, which are tentatively set as 10 d^{-1} and 10 kg COD/m^3, other parameters (inhibition constant of furfural ($K_{\mathrm{I,fu}}$, 2.11 kg COD/m^3), maximum specific uptake rate of furfural ($k_{\mathrm{m,fu}}$, 10 d^{-1}), half-saturation coefficient of furfural ($K_{\mathrm{s,fu}}$, 10 kg COD/m^3)) come from values reported by Raya and Ghimire (2022) and Liu et al. (2017). All other parameters not mentioned were set to the default values of the initial ADM1 (Batstone et al., 2002).

2.4.3. Parameter estimation

In AD simulations with lignocellulosic substrates, the parameters related to substrate hydrolysis were generally more sensitive, since hydrolysis is considered the rate-limiting step (Zhao et al., 2009; Li et al., 2021). Accordingly, lignocellulosic hydrolysis-related kinetic parameters ($k_{\mathrm{hyd,RHF}}$, $k_{\mathrm{hyd,SHF}}$, $K_{\mathrm{hyd,RHF}}$, and $K_{\mathrm{hyd,SHF}}$) and new furfural degradation-related parameters ($k_{\mathrm{m,fu}}$, $k_{\mathrm{m,fua}}$, $K_{\mathrm{I,fu}}$, $K_{\mathrm{s,fu}}$, and $K_{\mathrm{s,fua}}$) were estimated preferentially. The parameter bank was gradually expanded until the model outputs reached convergence criteria as estimated using Eq. (6):

$$\chi^2(p) = \sum_{\mathrm{i=1}}^{\mathrm{n}}\left(\frac{\mathrm{y_i}(p)-y_{\mathrm{meas,i}}}{\delta_{\mathrm{meas,i}}}\right)^2 \quad (6)$$

where y_i (p) and $y_{\mathrm{meas,i}}$ refer to the estimated model value and experimentally measured value of the i-th data point, respectively, and $\delta_{\mathrm{meas,i}}$ is the standard deviation.

3. Results and discussion

3.1. Batch experimental results and discussion

Fig. 1 shows details of the daily methane production and methane yield for batch anaerobic co-digestion of SEPW and CM at different mixing ratios. No methanogenesis was observed in $T_{control}$ treatment. All reactors except $T_{control}$ start-up immediately on the first day of AD, attributed to the presence of some soluble sugars and small molecule organic acids in the SEPW rapidly utilized by microorganisms (Li et al., 2021). In particular, maximum daily methane production values of T-1, −2, −3 and −4 were 232.2 (the 3rd day), 276.9 (the 3rd day), 363.5 (the 4th day), and 274.1 (the 6th day) mL CH_4/d, respectively, which not only had remarkable delay in time but also evident fluctuations in value. A possible reason for those significant delays is that the initial concentration of furfural in the reactor climbed from 0.20 (0.12) to 0.77 (0.46)

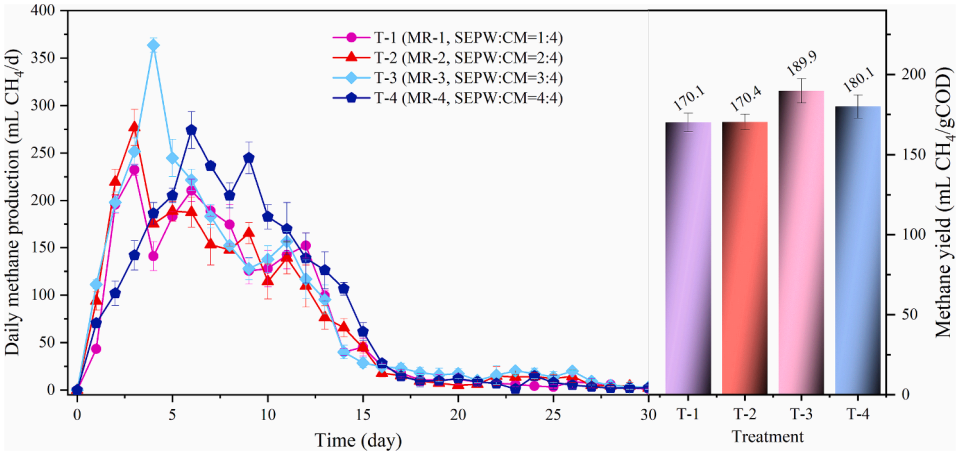

Fig. 1. Daily methane production and methane yield of batch anaerobic co-digestion of SEPW and CM at different mixing ratios.

kg COD/m^3 (g/L) with an increase in the amount of SEPW, which resulted in a progressively increasing inhibition on microbial growth (Ghasimi et al., 2016). In addition, methane yields of the four treatments ranged from 170.1 (T-1) to 189.9 (T-3) mL CH_4/g COD. The relatively high methane yield in T-3 suggested the optimum mixing ratio of SEPW to CM was 3:4 (3:37, based on dry weight).

3.2. Simulation of batch experiments

3.2.1. Model calibration

The cumulative methane production data from batch experiments T-1, −2, −3, and −4 were used for model calibration and parameter estimation in turn. The post-optimized model parameters and the fitting performance of the calibrated models (CT-1, −2, −3, and −4) are presented in Table 3. The χ^2 of the batch calibration groups ranged from 0.013 to 0.035, all of which <0.05, which confirmed the convergence standard was reached. (Zhao et al., 2019). The disintegration rate coefficients (k_{dis}) for the four calibration treatments slipped from an initial 0.50 d^{-1} to a range of 0.16–0.19 d^{-1}, which indicated a slower CM breakdown. The rate coefficient k_{dis}, which characterizes the only step in ADM1 that does not involve microorganisms, is highly substrate-dependent, with lignocellulosic biomass typically exhibiting lower k_{dis} values due to its granularity and recalcitrance because of its dense structure (Li et al., 2021). In contrast, Shi et al. (2014) reported a higher k_{dis} (0.362 d^{-1}) for CM in a study of CM co-digestion with spent mushroom substrate, while Bułkowska et al. (2015) proposed a slightly lower k_{dis} (0.10 d^{-1}) for the co-digestion of maize silage and CM. Regarding the hydrolysis of RHF and SHF fractions, $k_{hyd,RHF}$ and $k_{hyd,SHF}$ were estimated as 4.02–4.17 d^{-1} and 1.58–2.72 d^{-1} respectively, based on their respective initial values of 9.68 and 2.41 d^{-1}. Meanwhile, $K_{hyd,RHF}$ and $K_{hyd,SHF}$ were adjusted from initial values of 0.05 and 0.05 kg COD/m^3 to ranges of 0.68–0.97 kg COD/m^3 and 0.78–0.91 kg COD/m^3, respectively. Both the decrease in the k-factor and the increase in the K-factor for the SHF and RHF fractions indicated a significant decrease in hydrolysis reactions due to the microbial toxicity of furfural. Compared with an initial 10.00 d^{-1} derived from Liu et al. (2017), a relatively high average $k_{m,fu}$ of 20.53 d^{-1} was optimized from the batch calibration groups in this study. This apparent rise in $k_{m,fu}$ may be attributed to the fact that the initial value from Liu et al. (2017) characterized the aggregate rate of furfural conversion to acetic acid, whereas the optimized $k_{m,fu}$ in this study described the stepwise rate of furfural degradation to furoic acid. The adjusted $k_{m,fua}$ (average 3.71 d^{-1}) was much lower than $k_{m,fu}$ (average 20.53 d^{-1}), consistent with Rivard and Grohmann (1991) that the conversion of furoic acid to acetic acid was the rate-limiting step in the anaerobic degradation of furfural. Particularly, it was previously established that the furfural inhibition constant ($K_{I,fu}$) was highly sensitive, and that fine-tuning it led to highly variable rates of methane production (Raya and Ghimire, 2022). $K_{I,fu}$ was positively correlated with microbial adaptabilities and inversely correlated with inhibitor toxicity. Compared with the initial value of 2.11 kg COD/m^3 derived from the AD system with aqueous pyrolysis liquid as a single substrate (Raya and Ghimire, 2022), the post-optimized $K_{I,fu}$ for the batch-stage increased to 2.47 kg COD/m^3, most likely due to the implementing of co-digestion, which not only diluted the inhibitor but also allowed microbes to thrive for greater inhibitor resistance. Furthermore, a CT-4-based parameter sensitivity analysis revealed that parameters for CM disintegration and hydrolysis, as well as those related to furfural degradation, were relatively sensitive to cumulative methane production. It is noteworthy that the sensitivity of $K_{I,fu}$ gradually increased during the first 8 days of AD and then rapidly decreases to zero. This may be due to the weakened toxicity of furfural in the system after the majority of furfural in SEPW is converted to furoic acid (see supplementary materials).

The fitting results of the experimentally measured and simulated (both calibrated and uncalibrated model outputs) cumulative methane production data of T-1, −2, −3 and −4 are shown in Fig. 2(a – d), respectively. The output values of the four calibrated models coincided perfectly with their measured data, with excellent goodness-of-fit-degrees (R^2) exceeding 0.990 that indicated the implementation of parameter estimation assigned appropriate magnitudes to those misaligned kinetic parameters listed in Table 3.

3.2.2. Model cross-validation

The models were validated using the leave-one-out (LOO) cross-validation, where a single treatment is left out of the calibration group and used to validate the model. This process was then repeated with a different treatment used for validation and so on until all treatments have been used for validation. The cross-validation results (VT-1, −2, −3, and −4) are reported in Table 3. Satisfactory R^2 values (0.959–0.984) confirmed the calibrated model predicted dynamic methanogenesis of different treatments. In addition, Fig. 2(a – d) show the cumulative methane production curve fitted by the calibration model matched well with the practical case regardless of treatment. These results indicated the batch-stage modified ADM1 optimized in this

Table 3
Summary of model calibration, cross-validation and model recalibration results.

Source	Types	Unit	Batch calibration				Batch validation				Semi-continuous recalibration	
			CT-1	CT-2	CT-3	CT-4	VT-1	VT-2	VT-3	VT-4	CR-1	CR-2
Kinetic parameters	k_{dis}	d^{-1}	0.17	0.16	0.19	0.18	0.18[a]	0.18[b]	0.17[c]	0.17[d]	0.18[e]	0.18[e]
	$k_{hyd,RHF}$	d^{-1}	4.02	4.05	4.17	4.11	4.11[a]	4.10[b]	4.06[c]	4.08[d]	4.09[e]	4.09[e]
	$k_{hyd,SHF}$	d^{-1}	1.58	1.65	2.72	2.31	2.23[a]	2.20[b]	1.85[c]	1.98[d]	2.07[e]	2.07[e]
	$K_{hyd,RHF}$	kg COD/m^3	0.68	0.97	0.72	0.82	0.84[a]	0.74[b]	0.82[c]	0.79[d]	0.80[e]	0.80[e]
	$K_{hyd,SHF}$	kg COD/m^3	0.91	0.78	0.81	0.88	0.82[a]	0.87[b]	0.86[c]	0.83[d]	0.85[e]	0.85[e]
	$k_{m,fu}$	d^{-1}	25.13	15.77	19.95	21.25	18.99[a]	22.11[b]	20.72[c]	20.28[d]	35.20[*]	37.11[#]
	$k_{m,fua}$	d^{-1}	7.16	2.28	2.83	2.55	2.55[a]	4.18[b]	4.00[c]	4.09[d]	3.71[e]	3.71[e]
	$K_{I,fu}$	kg COD/m^3	3.69	2.73	1.59	1.87	2.06[a]	2.38[b]	2.76[c]	2.67[d]	5.97[*]	6.13[#]
	$K_{s,fu}$	kg COD/m^3	10.51	8.80	9.12	9.92	9.28[a]	9.85[b]	9.74[c]	9.48[d]	9.01[*]	9.17[#]
	$K_{s,fua}$	kg COD/m^3	24.30	15.02	15.95	17.68	16.22[a]	19.31[b]	19.00[c]	18.42[d]	18.24[e]	18.24[e]
Fitting performance	χ^2	–	0.013	0.035	0.019	0.011	–	–	–	–	–	–
	R^2	–	0.997	0.990	0.996	0.998	0.959	0.975	0.967	0.984	–	–

[a] Average of CT-2, −3, and –4.
[b] Average of CT-1, −3, and –4.
[c] Average of CT-1, −2, and –4.
[d] Average of CT-1, −2, and –3; [e] Average of VT-1, −2, −3, and –4.
[*] Parameter values derived from recalibration based on R-2.
[#] Parameter values derived from recalibration based on R-1.

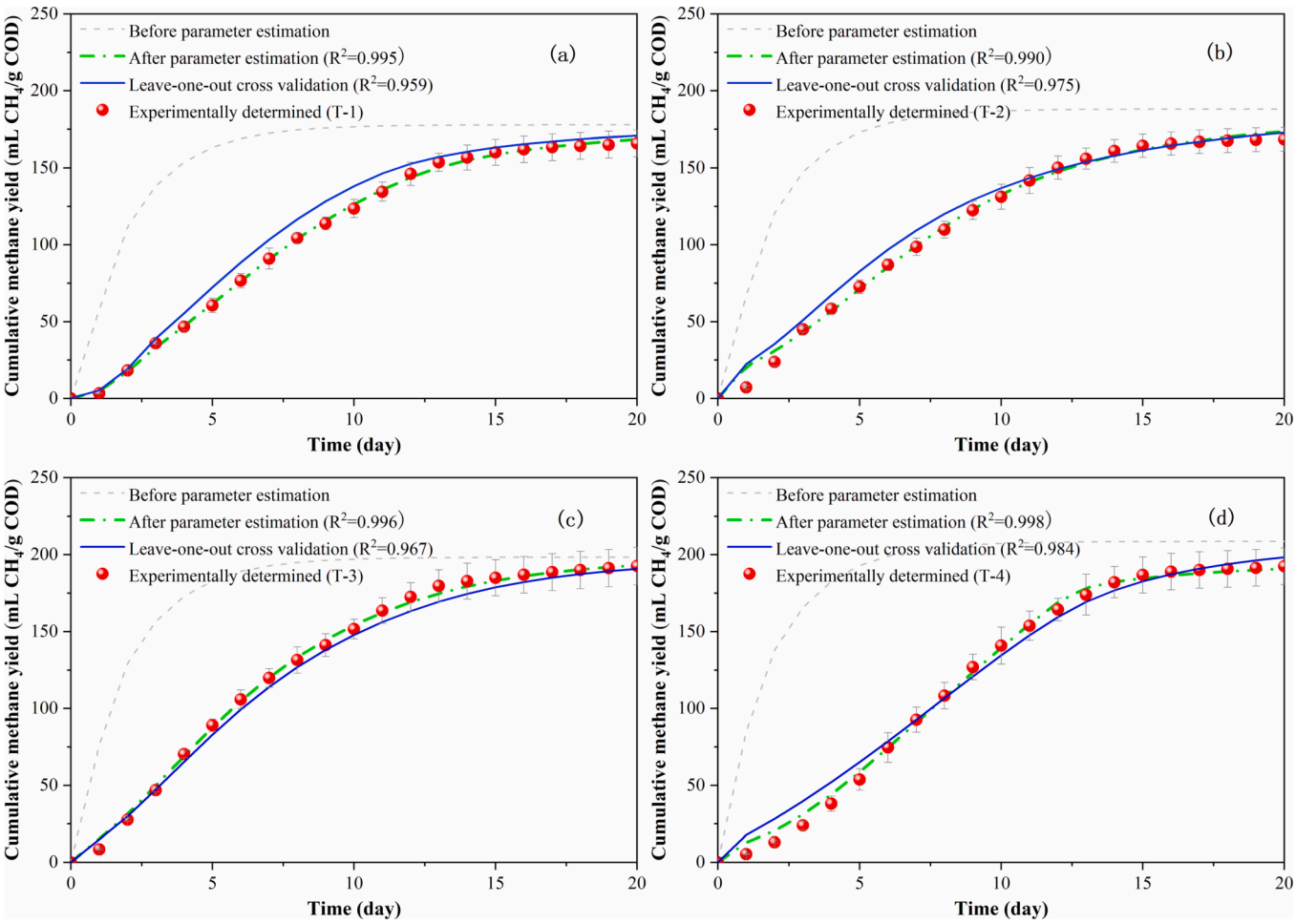

Fig. 2. Measured cumulative methane yield, model output value before and after parameter calibration and LOO cross-validation results of (a) T-1 (model calibration with T-2, −3, and −4), (b) T-2 (model calibration with T-1, −3, and −4), (c) T-3 (model calibration with T-1, −2, and −4), and (d) T-4 (model calibration with T-1, −2, and −3).

study properly simulated the batch co-digestion of SEPW and CM at different mixing ratios, and implied the assumptions and adaptations proposed for model establishment (such as the introduction of furoic acid as an intermediate in furfural degradation) were reasonable.

3.3. Semi-continuous experimental results and discussion

Fig. 3(a and b) show the methane production curves of R-1 and R-2, respectively. During the first 25 days of the first phase (HRT = 40 d), methane production of R-1 gradually climbed from 0 to 2.36 NL CH_4/d (equivalent to 112.90 mL/g COD·d) and remained constant with slight fluctuations from day 25 to 40. This indicated the successful start-up and normal progression of the semi-continuous experiment. In the second phase (41–70 days), HRT was directly adjusted from the initial 40 d to 20 d, whereas the methane yield of R-1 stabilized around 4.22 NL CH_4/d (equivalent to 102.94 mL/g COD·d) after a brief strong fluctuation. After lowering the HRT to 10 d (71–85 days), methane production of R-1 rose again and stabilized ~6.46 NL CH_4/d (equivalent to 74.05 mL/g COD·d). Compared with the first phase, the OLR of R-1 in the third phase increased by a factor of three (from 2.65 to 10.60 g COD/(L·d)), while the methane production rate increased by only ~1.7 times (from 2.36 to 6.46 NL CH_4/d). This result indicated the highly recalcitrant components in CM (e.g., lignocellulose) were insufficiently digested with shortened residence times (Li et al., 2021). The methanogenesis trends of R-2 in the first and second phases were basically the same as that of R-1. Distinctively, an extremely rapid increase in methane production rate similar to that of R-1 occurred during the first four days of the third phase of R-2, however, unlike R-1, the methane yield was not maintained but dropped.

to the second phase levels of R-2 (~4.90 NL CH_4/d) until the end of the experiment. The most likely reason for this was that with the increase of OLR, the infusion of furfural exceeded the upper-limit of microbial detoxification, and the accumulation of overloaded furfural at a certain concentration led to microbial inhibition.

3.4. Simulation of semi-continuous experiments

3.4.1. Simulation by batch-stage calibrated model

The simulation results of semi-continuous experiments R-1 and R-2 by batch-stage calibrated ADM1 are shown in Fig. 3(a and b). Overall, the batch-stage model predicted methanogenesis during stable periods (e.g., 25–40 days and 47–70 days). Meanwhile, the model also made unsatisfactory predictions, primarily manifested in three stages: the experimental start-up (1–24 days), the HRT sudden drop (41–46 days), and the inhibitor overload stages (71–85 days, the entire third phase). Similarly, Zhao et al. (2019) also reported simulation misalignments in the start-up and the HRT sudden drop stages and used a modified ADM1 to model AD of food waste under batch and semi-continuous modes. As suggested by Zhao et al. (2019), the ADM1 established in this study did not account for the gradual adaptation process of microorganisms to substrates in the start-up stage and the strong impact on microbial activity caused by the rapid feed load increase in the HRT adjustment stage, which may explain prediction inaccuracies in these two stages. Regarding the simulation misalignments in the third phase of the semi-continuous experiment,

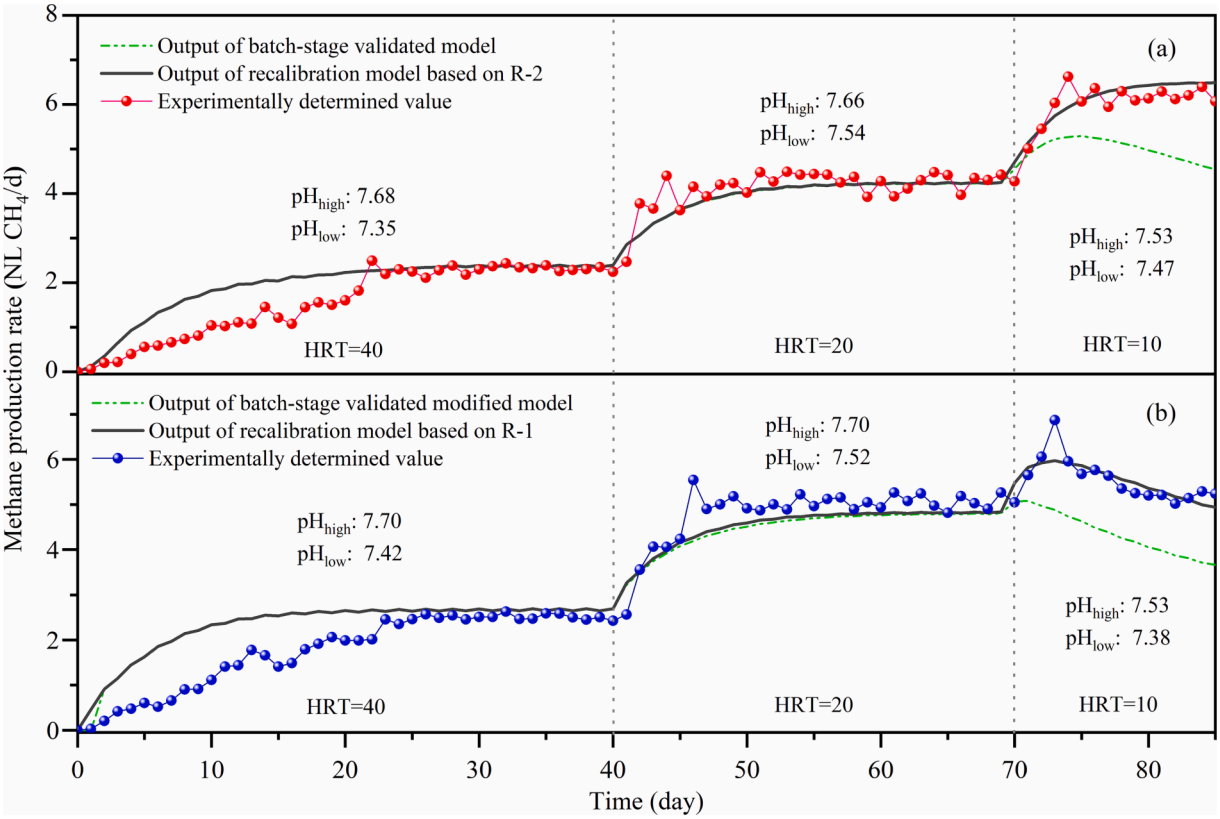

Fig. 3. Methane production rate and pH changes of (a) R-1 (with MR-2 as substrate, SEPW:CM = 2:4) and (b) R-2 (with MR-4 as substrate, SEPW:CM = 4:4) during the semi-continuous experimental period; Simulation results of batch-stage model and cross-validation results of recalibration model of (a) R-1 (recalibration based on R-2) and (b) R-2 (recalibration based on R-1).

inhibition of furfural as predicted by the batch-stage model did not occur or occurred with a lower intensity in the actual semi-continuous experiment. The theory proposed by Raya and Ghimire (2022) and Wen et al. (2020) explains this well, who emphasized that microbes adapted to the inhibitor and, thus the inhibitory effect of the inhibitor decreased over time in a continuous AD reactor. These results suggested the batch-stage model was somewhat unusable in simulating semi-continuous experiments because of its inability to predict the inhibition strength. It can be inferred that the inappropriate assignment of kinetic parameters related to the degradation of furfural ($K_{I,fu}$, $k_{m,fu}$, and $K_{s,fu}$) is probably the main reason for this result, because the inhibition of furfural acid on methanogens is far lower than furfural (Ghasimi et al., 2016; Sun et al., 2020).

3.4.2. *Model recalibration and revalidation*

To minimize the simulation gap of the batch-stage model at high inhibitor concentrations and evaluate differences in furfural tolerance between batch and semi-continuous AD systems, the furfural degradation-related parameters ($K_{I,fu}$, $k_{m,fu}$, and $K_{s,fu}$) in the batch-stage model were recalibrated and reverified using semi-continuous experimental data while maintaining the other parameters. The cross-validation was implemented again at this stage. The model was recalibrated based on methane production data from R-1 and R-2. As shown in Table 3, after recalibration, $K_{I,fu}$ (from 2.47 to 6.05 kg COD/m^3) and $k_{m,fu}$ (from 20.53 to 36.16 d^{-1}) increased significantly, while $K_{s,fu}$ (from 9.59 to 9.09 kg COD/m^3) decreased slightly, and all confirmed that longer acclimatization strengthen semi-continuous system tolerances to inhibitors (Wen et al., 2020). The recalibration model cross-validation results by R-1 (with parameters from R-2 recalibration) and R-2 (with parameters from R-1 recalibration) are shown in Fig. 3(a) and (b), respectively. The recalibrated model output values correspond well to the suppressed methanogenic process of the third phase of R-1 and R-2, which indicated the recalibrated model compensated for the lack of predictive power of the batch-stage model at high inhibitor levels, and predicts the inhibition intensity of furfural well.

Moreover, the batch-stage and recalibration models had almost similar model output values during the first two phase simulations of the semi-continuous experiment. The simulation results of the first two semi-continuous experiment phases were not significantly influenced by a large adjustment of the parameters related to furfural degradation. This indicated that other factors (such as hydrolysis of lignocellulose) rather than furfural inhibition dominated the methane production rate during the first two phases of the semi-continuous experiment. However, methanogenesis in a mutational environment (such as a start-up stage or a HRT sudden drop stage) was not accurately represented by either the batch-stage model or the semi-continuous stage recalibrated model. This limitation needs to be addressed in the future.

4. Conclusions

Results from batch and semi-continuous experiments indicated that SEPW and CM co-digestion strategies at appropriate mixing ratios are feasible. The extended ADM1 established in this study emphasized the degradation and inhibition properties of furfural and accurately simulated the batch co-digestion of SEPW and CM ($R^2 \geq 0.959$). The recalibrated model satisfactorily matched the methanogenesis behavior in the stable and high inhibitor loading stages of both semi-continuous reactors, which revealed the semi-continuous system tolerated furfural better than the batch system. This study provides a basis for the anaerobic treatment and mathematical simulation of furfural-rich substrates.

CRediT authorship contribution statement

Pengfei Li: Investigation, Data curation, Formal analysis, Writing – original draft. **Xinyu Wei:** Methodology, Software, Data curation. **Ming**

Wang: Investigation, Validation, Writing – review & editing. **Di Liu:** Methodology, Software, Data curation. **Jie Liu:** Investigation, Supervision. **Zhanjiang Pei:** Writing – review & editing. **Fengmei Shi:** . **Su Wang:** Writing – review & editing. **Xin Zuo:** Methodology, Data curation. **Dan Li:** Formal analysis. **Hongjiu Yu:** Writing – review & editing. **Nan Zhang:** Writing – review & editing. **Qiuyue Yu:** Writing – review & editing. **Yifei Luo:** Writing – review & editing.

Declaration of Competing Interest

The authors declare that they have no known competing financial interests or personal relationships that could have appeared to influence the work reported in this paper.

Data availability

Data will be made available on request.

Acknowledgments

Funding: This work was supported by the National Natural Science Fund of China (52200151 and U21A20162), the China Postdoctoral Science Fund (2022T150200, 2021M693834), the Postdoctoral Science Fund of Heilongjiang Province (LBH-TZ2118 and LBH-Q21174), Heilongjiang Provincial Research Institutes Special Business Expenses (CZKYF2021-2-C003, CZKYF2022-1-B029, and CZKYF2022-1C002) and Innovation Project of Heilongjiang Academy of Agricultural Sciences (2021YYYF001).

Appendix A. Supplementary data

Supplementary data to this article can be found online at https://doi.org/10.1016/j.biortech.2023.129086.

References

Akassou, M., Kaanane, A., Crolla, A., Kinsley, C., 2010. Statistical modelling of the impact of some polyphenols on the efficiency of anaerobic digestion and the co-digestion of the wine distillery wastewater with dairy cattle manure and cheese whey. Water Sci. Technol. 62 (3), 475–483. https://doi.org/10.2166/wst.2010.235.

APHA, 2005. Standard Method for Examination of Water and Wastewater, 21st ed. AWWA, WPCF, Washington.

Batstone, D.J., Keller, J., Angelidaki, I., Kalyuzhnyi, S.V., Pavlostathis, S.G., Rozzi, A., Sanders, W.T., Siegrist, H., Vavilin, V.A., 2002. The IWA anaerobic digestion model No. 1 (ADM1). Water sci. Technol. 45, 65–73. https://doi.org/10.2166/wst.2002.0292.

Boopathy, R., Bokang, H., Daniels, L., 1993. Biotransformation of furfural and 5-hydroxymethyl furfural by enteric bacteria. J. Ind. Microbiol. 11, 147–150. https://doi.org/10.1007/BF01583715.

Bułkowska, K., Białobrzewski, I., Gusiatin, Z.M., Klimiuk, E., Pokój, T., 2015. ADM1-based modeling of anaerobic codigestion of maize silage and cattle manure – calibration of parameters and model verification (part II). Arch. Environ. Prot. 41, 20–27. https://doi.org/10.1515/aep-2015-0027.

Chai, A., Wong, Y.-S., Ong, S.-A., Aminah Lutpi, N., Sam, S.-T., Kee, W.-C., Ng, H.-H., 2021. Haldane-Andrews substrate inhibition kinetics for pilot scale thermophilic anaerobic degradation of sugarcane vinasse. Bioresour. Technol. 336, 125319 https://doi.org/10.1016/j.biortech.2021.125319.

Chi, C., Zhang, Z., Chang, H., Jameel, H., 2009. Determination of Furfural and Hydroxymethylfurfural Formed from Biomass Under Acidic Conditions. J. Wood Chem. Technol. 29, 265–276. https://doi.org/10.1080/02773810903096025.

Dareioti, M.A., Dokianakis, S.N., Stamatelatou, K., Zafiri, C., Kornaros, M., 2010. Exploitation of olive mill wastewater and liquid cow manure for biogas production. Waste Manag. 30, 1841–1848. https://doi.org/10.1016/j.wasman.2010.02.035.

Emebu, S., Pecha, J., Janáčová, D., 2022. Review on anaerobic digestion models: Model classification & elaboration of process phenomena. Renew. Sustain. Energy Rev. 160, 112288 https://doi.org/10.1016/j.rser.2022.112288.

Fezzani, B., Cheikh, R.B., 2009. Extension of the anaerobic digestion model No. 1 (ADM1) to include phenolic compounds biodegradation processes for the simulation of anaerobic co-digestion of olive mill wastes at thermophilic temperature. J. Hazard. Mater. 162, 1563–1570. https://doi.org/10.1016/j.jhazmat.2008.06.127.

Ghasimi, D.S.M., Aboudi, K., de Kreuk, M., Zandvoort, M.H., van Lier, J.B., 2016. Impact of lignocellulosic-waste intermediates on hydrolysis and methanogenesis under thermophilic and mesophilic conditions. Chem. Eng. J. 295, 181–191. https://doi.org/10.1016/j.cej.2016.03.045.

Girolamo, G.D., Grigatti, M., Barbanti, L., Angelidaki, I., 2013. Effects of hydrothermal pre-treatments on Giant reed (Arundo donax) methane yield. Bioresour. Technol. 147, 152–159. https://doi.org/10.1016/j.biortech.2013.08.006.

Kafle, G.K., Kim, S.-H., 2012. Kinetic Study of the Anaerobic Digestion of Swine Manure at Mesophilic Temperature: A Lab Scale Batch Operation. J. Biosyst. Eng. 37, 233–244. https://doi.org/10.5307/JBE.2012.37.4.233.

Karki, R., Chuenchart, W., Surendra, K.C., Shrestha, S., Raskin, L., Sung, S., Hashimoto, A., Khanal, S.K., 2021. Anaerobic co-digestion: Current status and perspectives. Bioresour. Technol. 330, 125001 https://doi.org/10.1016/j.biortech.2021.125001.

Ketsub, N., Whatmore, P., Abbasabadi, M., Doherty, W.O.S., Kaparaju, P., O'Hara, I.M., Zhang, Z., 2022. Effects of pretreatment methods on biomethane production kinetics and microbial community by solid state anaerobic digestion of sugarcane trash. Bioresour. Technol. 352, 127112 https://doi.org/10.1016/j.biortech.2022.127112.

Koch, K., Lübken, M., Gehring, T., Wichern, M., Horn, H., 2010. Biogas from grass silage – Measurements and modeling with ADM1. Bioresour. Technol. 101, 8158–8165. https://doi.org/10.1016/j.biortech.2010.06.009.

Lane, J.H., Eynon, L., 1924. Estimation of sugar in urine by means of Fehling's solution with methylene blue as internal indicator. The Analyst 49, 366. https://doi.org/10.1039/an9244900366.

Li, P., Pei, Z., Liu, D., Shi, F., Wang, S., Li, W., Sun, Y., Liu, J., Gao, Y., Yu, Q., 2021. Application of Anaerobic Digestion Model No. 1 for modeling anaerobic digestion of vegetable crop residues: Fractionation of crystalline cellulose. J. Clean. Prod. 285, 124865 https://doi.org/10.1016/j.jclepro.2020.124865.

Li, H., Wang, C., Chen, X., Xiong, L., Guo, H., Yao, S., Wang, M., Chen, X., Huang, C., 2022. Anaerobic digestion of rice straw pretreatment liquor without detoxification for continuous biogas production using a 100 L internal circulation reactor. J. Clean. Prod. 349, 131450.

Liu, B., Ngo, V.A., Terashima, M., Yasui, H., 2017. Anaerobic treatment of hydrothermally solubilised sugarcane bagasse and its kinetic modelling. Bioresour. Technol. 234, 253–263. https://doi.org/10.1016/j.biortech.2017.03.024.

Monlau, F., Sambusiti, C., Barakat, A., Guo, X.M., Latrille, E., Trably, E., Steyer, J.-P., Carrere, H., 2012. Predictive Models of Biohydrogen and Biomethane Production Based on the Compositional and Structural Features of Lignocellulosic Materials. Environ. Sci. Technol. 46, 12217–12225. https://doi.org/10.1021/es303132t.

Montane, D., Farriol, X., Salvado, J., Jollez, P., Chornet, E., 1998. Application of steam explosion to the fractionation and rapid vapor-phase alkaline pulping of wheat straw [J]. Biomass Bioenergy 14 (3), 261–276. https://doi.org/10.1016/S0961-9534(97)10045-9.

Raya, D., Ghimire, N., Flatabø, G.Ø., Bergland, W.H., 2022. Anaerobic Digestion of Aqueous Pyrolysis Liquid in ADM1. September 21-23, Virtual Conference, Finland, pp. 458–464. doi: 10.3384/ecp21185458.

Rivard, C. j., Grohmann, K., 1991. Degradation of furfural (2- furaldehyde) to methane and carbon dioxide by an anaerobic consortium. Appl. Biochem. Biotechnol. 28–29, 285–295. doi: 10.1007/BF02922608.

Ruiz, H.A., Galbe, M., Garrote, G., Ramirez-Gutierrez, D.M., Ximenes, E., Sun, S.-N., Lachos-Perez, D., Rodríguez-Jasso, R.M., Sun, R.-C., Yang, B., Ladisch, M.R., 2021. Severity factor kinetic model as a strategic parameter of hydrothermal processing (steam explosion and liquid hot water) for biomass fractionation under biorefinery concept. Bioresour. Technol. 342, 125961 https://doi.org/10.1016/j.biortech.2021.125961.

Sarker, T.R., Pattnaik, F., Nanda, S., Dalai, A.K., Meda, V., Naik, S., 2021. Hydrothermal pretreatment technologies for lignocellulosic biomass: A review of steam explosion and subcritical water hydrolysis. Chemosphere 284, 131372. https://doi.org/10.1016/j.chemosphere.2021.131372.

Shi, X.-S., Yuan, X.-Z., Wang, Y.-P., Zeng, S.-J., Qiu, Y.-L., Guo, R.-B., Wang, L.-S., 2014. Modeling of the methane production and pH value during the anaerobic co-digestion of dairy manure and spent mushroom substrate. Chem. Eng. J. 244, 258–263. https://doi.org/10.1016/j.cej.2014.02.007.

Siddique, Md.N.I., Sakinah Abd Munaim, M., Zularisam, A.W., 2014. Mesophilic and thermophilic biomethane production by co-digesting pretreated petrochemical wastewater with beef and dairy cattle manure. J. Ind. Eng. Chem. 20, 331–337. doi: 10.1016/j.jiec.2013.03.030.

Sun, C., Liao, Q., Xia, A., Fu, Q., Huang, Y., Zhu, X., Zhu, X., Wang, Z., 2020. Degradation and transformation of furfural derivatives from hydrothermal pre-treated algae and lignocellulosic biomass during hydrogen fermentation. Renew. Sustain. Energy Rev. 131, 109983 https://doi.org/10.1016/j.rser.2020.109983.

Wang, N., Chen, H.Z., 2013. Manufacture of dissolving pulps from cornstalk by novel method coupling steam explosion and mechanical carding fractionation. Bioresour. Technol. 139, 59–65. https://doi.org/10.1016/j.biortech.2013.04.015.

Wen, C., Moreira, C.M., Rehmann, L., Berruti, F., 2020. Feasibility of anaerobic digestion as a treatment for the aqueous pyrolysis condensate (APC) of birch bark. Bioresour. Technol. 307, 123199 https://doi.org/10.1016/j.biortech.2020.123199.

Yu, Y., Wu, J., Ren, X., Lau, A., Rezaei, H., Takada, M., Bi, X., Sokhansanj, S., 2022. Steam explosion of lignocellulosic biomass for multiple advanced bioenergy processes: A review. Renew. Sustain. Energy Rev. 154, 111871 https://doi.org/10.1016/j.rser.2021.111871.

Zhao, X., Li, L., Wu, D., Xiao, T., Ma, Y., Peng, X., 2019. Modified Anaerobic Digestion Model No. 1 for modeling methane production from food waste in batch and semi-continuous anaerobic digestions. Bioresour. Technol. 271, 109–117. https://doi.org/10.1016/j.biortech.2018.09.091.

Zhao, B.-H., Yue, Z.-B., Ni, B.-J., Mu, Y., Yu, H.-Q., Harada, H., 2009. Modeling anaerobic digestion of aquatic plants by rumen cultures: Cattail as an example. Water Res. 43 (7), 2047–2055. https://doi.org/10.1016/j.watres.2009.02.006.